RAM ROBOTICS AND MECHATRONICS

ENERGETIC CONSISTENCY OF COSSERAT ROD SIMULATIONS

R.F. (Ruben) Ufkes

MSC ASSIGNMENT

Committee:
prof. dr. ir. S. Stramigioli
Y.P. Wotte, MSc
dr. ir. R.A.M. Rashad
dr. ir. G. Meinsma

September, 2024

063RaM2024
Robotics and Mechatronics
EEMCS
University of Twente
P.O. Box 217
7500 AE Enschede
The Netherlands

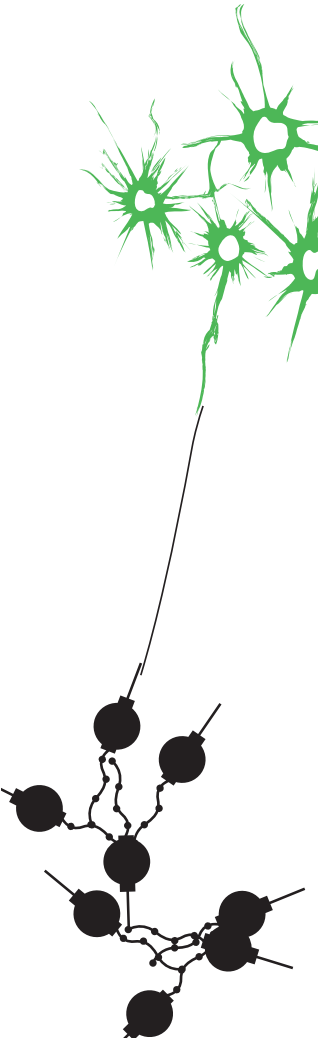

UNIVERSITY OF TWENTE. | TECHMED CENTRE UNIVERSITY OF TWENTE. | DIGITAL SOCIETY INSTITUTE

Abstract

In this thesis, the energetic behavior of a Cosserat rod is examined. The Cosserat rod theory is a mathematical framework used to model the mechanics of slender, flexible structures. It was chosen to go for a strain-parameterized approach, which focuses on describing the rod's deformation in terms of its internal strains rather than its absolute position and orientation. The dynamics of the Cosserat rod were formulated using the least action principle, a concept in physics that states that the path a system takes between two points is the one that minimizes the action integral. An interesting observation was made when trying to reconstruct the rod's geometry (configuration) through the strain. We have noticed that this process is not straightforward and requires the use of the Magnus expansion. The Magnus expansion is a mathematical technique used to solve differential equations with a non-constant matrix, particularly those involving non-commuting operators, which is needed to accurately represent the rod's configuration in space. The continuous kinematics and dynamics equations were reduced by assuming that the strain field can be approximated through a finite set of basis functions and their generalized coordinates. Then the reduced equations were discretized through the Gauss quadrature method and the Magnus series was approximated by the Zanna collocation method. A variety of simulations were executed through the SoRoSim toolbox in order to see the impact of different bases functions and Magnus expansion approximation orders. Although the toolbox shows flaws in calculating the strain energy, it was verified that all the other energies were calculated correctly. It was therefore chosen to assume that the total energy of the system is zero and through the energy balance the elastic potential energy was retrieved. When comparing local FEMlike basis functions with global Chebyshev polynomial functions, it is shown that the kinetic and gravitational potential energies were the same but the elastic potential energy differs. The effects on the choice of bases order are also shown with relatively large energy differences between the two high order and one low order Chebyshev polynomials, but the energy difference between the high order bases was minimal. There was no energy differences shown between Chebyshev and Legendre polynomials of the same order. This could be because the polynomial families have a lot of the same characteristics. Lastly, when altering the Zanna approximation order all the energies show a difference.

Contents

1 Introduction

The study of soft robotics is a relatively new field of interest in the robotics community, although the starting point of the first "soft robot" could be considered already around the time before the well-known industrial robot made its introduction. This first soft robot was in the form of a prosthetic or "artificial muscle", a term coined by its inventor Joseph Laws McKibben [1]. With this pneumatic device, the muscle contracts axially when pressurized air expands the muscle radially, causing the surrounding shell made as a breaded mesh to shorten and generate a pulling force. Dr. McKibben, an engineer and atomic physicist also known for his work on the Manhattan project, made this invention with the hope it would aid polio patients suffering from paralysis.

Yet it was only since the year 2010 that the words "soft robotics" became popular and that the field started to receive proper attention[2]. There are multiple definitions for the term "soft robotics", but they have all in common that a key feature is the use of soft materials.

The community frequently draws its inspiration for design from nature, since animals often can perform certain tasks efficiently due to their flexible body parts [3]. For instance, Figure 1 shows how the tentacles of a jellyfish used to hold prey has influenced the design of a tentacle gripper which is able to hold objects of various shapes and sizes.

(a) Image of a jellyfish [4]

(b) A gripper inspired on the anatomy of a jellyfish [5]

Figure 1: An example of drawing inspiration from nature

During the design phase, one important aspect is the ability of simulating the system in order to predict its behaviour when it is deployed into a real world environment. This identifies the need of proper simulation software. Simulation of a soft robotic system goes through the use of a simulation model. This model should capture the aspects of interest from the system and is often a simplification of the real design.

The structure of soft robotics is a shift from its traditional counterpart with finite degrees of freedom since soft robot structures have an infinite amount of degrees of freedom. This immediately shows one of the challenges faced in this field. Namely, how to approach these infinite degrees of freedom for such soft structures in case of design and simulation.

1.1 Problem statement

When looking at academic literature papers that discusses the formulation of the Cosserat beam model, often the results that are shown are of the model reaching a setpoint in 3-dimensional Euclidean space. Although this might be interesting, the literature often lack to properly show the affects the modelling choices have on the energy balance.

In this thesis, we seek to explore the theoretical- and simulation aspects of the Cosserat rod with the focus on how the geometry is reconstructed and what the effects are by choosing certain simulation parameters.

1.2 Related work

Introduced by the brothers Eugène and François Cosserat ([6]), the theory of Cosserat rods is a generalization of Kirchoff rods which apart from bending and torsion it additionally considers stretching and shearing thus capturing more behaviour of elastic deformation of a rod [7]. The key assumption for a Cosserat model is that the model is split up into an infinite amount of rigid cross-sections and the length of the rod is much larger than the radius.

The Cosserat beam model is a well known model in the soft robotics community. Compared to other rod models, the Cosserat rod captures all the deformation modes (e.g. bending, shearing, twisting) with the key assumption that the length of the rod is much longer than its radius.

Common ways to describe the balancing laws of a Cosserat rod is through a classical method of global parametrization approach or by a geometric Screw theory formulation. Screw theory formulation has multiple advantages over its classical counterpart. The main benefit is the implementation of a global parameterization-free formulation of the equations of motion, avoiding the need for 3 or more parameters (e.g. Euler Angles and quaternions) to define angular motion. This approach gets rid of the highly nonlinear equations and singularities found in the classical method, while better reflecting the dynamics inherent symmetries. By using Lie groups (specifically the SO(3) and SE(3) groups) to express the equations of motion globally, it gets rid of these issues without assuming any local parametrization [8]. Further explanation of the two methods can be found in [9].

In [9], the continuum dynamics of the Cosserat rod is derived through Hamilton's least action principle whereas in [10] the dynamics are derived through a Newton-Euler formulation. It should be noted that both methods are equivalent to each other, meaning that the obtained equations of motion are the same.

The main focus of the discretization of the continuum model is to reduce the infinite strain state of a rod configuration. This is done for instance by a finite-dimensional model order projection in [10] or by a piece-wise constant deformation [9].

1.3 Thesis contribution

This thesis helps to contribute to a better analyses of the energetic structure and how the choice of model order reduction and discretization influences this.

1.4 Research questions

In order to do so properly, the following research question has been formulated.

How is the energetic consistency of the Cosserat rod model affected by discretization?

To answer this, we split the research question up into two sub-questions:

1. How can the continuous model be formulated?

2. How can the model be discretized?

1.5 Thesis structure

We begin by introducing some notation and mathematics which are used throughout this thesis. These are found in the Preliminaries (chapter 2). After that, the continuous model (its kinematics and dynamics) of the Cosserat is defined in chapters 3 and 4 respectively. In order to use this model, it needs to be reduced and discretized so it later can be implemented as a simulation. This the model order reduction is explained in chapter 5 and the discretization process is explained in chapter 6. The simulation setup is stated in chapter 7 and the results are then shown in chapter 8. Lastly, conclusions and recommendations for future work are mentioned in chapter 9.

2 Preliminaries

2.1 Differential geometry

2.1.1 Manifolds

Definition 1 Let $\mathcal{M}$ be a topological space. $\mathcal{M}$ is an n-dimensional differentiable manifold if:

1. $\mathcal{M}$ is a second-countable Hausdorff space.

2. There exists a collection of pairs (U_α, ϕ_α), called charts, where: $U_\alpha \subseteq \mathcal{M}$ is an open set $\phi_\alpha : U_\alpha \to V_\alpha \subseteq \mathbb{R}^n$ is a homeomorphism $\bigcup_\alpha U_\alpha = \mathcal{M}$

3. For any two charts (U_α, ϕ_α) and (U_β, ϕ_β) with $U_\alpha \cap U_\beta \neq \emptyset$, the transition map: $\phi_\beta \circ \phi_\alpha^{-1} : \phi_\alpha (U_\alpha \cap U_\beta) \to \phi_\beta (U_\alpha \cap U_\beta)$ is differentiable.

The collection of all such charts (U_α, ϕ_α) is called an atlas for $\mathcal{M}$.

2.1.2 Tangent spaces

Definition 2 Let $\mathcal{M}$ be a smooth (differentiable) manifold and $p \in \mathcal{M}$ be a point on the manifold. The tangent space $T_p\mathcal{M}$ at point p is defined as: $T_p\mathcal{M} = \{\gamma'(0) \mid \gamma : (-\epsilon, \epsilon) \to \mathcal{M} \text{ is a smooth curve with } \gamma(0) = p\}$ Where:

$\cdot\ \gamma : (-\epsilon, \epsilon) \to \mathcal{M}$ is a smooth curve on $\mathcal{M}$ passing through p at $t = 0$

$\cdot\ \gamma'(0)$ represents the velocity vector of the curve at $t = 0$ Equivalently, using a local coordinate chart (U, ϕ) around p, we can define the tangent space as:

$$T_p\mathcal{M} := \left\{ \sum_{i=1}^{n} a_i \left. \frac{\partial}{\partial x^i} \right|_p \mid a_i \in \mathbb{R} \right\}$$

Where $\frac{\partial}{\partial x^i}|_p$ are the basis vectors of the tangent space and n is the dimension of the manifold.

2.1.3 Bundles

Definition 3 Let $\mathcal{M}$ be a smooth manifold. A Tangent bundle is represented as:

$$\begin{aligned} T\mathcal{M} &:= \bigcup_{p \in \mathcal{M}} T_p\mathcal{M} \\ &= \{(p, y) \mid p \in \mathcal{M}, y \in T_p\mathcal{M}\} \end{aligned} \tag{2.1}$$

Definition 4 Let $\mathcal{M}$ again be a smooth manifold. The cotangent bundle of $\mathcal{M}$, denoted $T^*\mathcal{M}$, is defined as:

$$T^*\mathcal{M} := \bigcup_{p \in M} T_p^*\mathcal{M}$$

Where $T_p^*\mathcal{M}$ is the cotangent space at point p, which is the dual vector space to the tangent space $T_p\mathcal{M}$. A dual vector space $V^* : V \mapsto \mathbb{R}$, is defined as the set of all linear functionals on a vector space V.

Given a vector space E, we will generally denote the space of E-valued differential k-forms by

$$\Omega^k(\mathcal{M}; E) := \Gamma\left(\Lambda^k T^*\mathcal{M}\right) \tag{2.2}$$

With $\Lambda^k T^*\mathcal{M}$ being the cotangent bundle with exterior power k and an element $\omega \in \Gamma\left(\Lambda^k T^*\mathcal{M}\right)$ representing a section (a field of k-forms) of that bundle.

2.2 Lie Theory

2.2.1 Lie group fundamentals

Definition 5 A group is an ordered pair $(G, \cdot)$,where G is a set and $\cdot : G \times G \to G$ is a binary operation on G, satisfying the following axioms:

1. Associativity: For all $a, b, c \in G, (a \cdot b) \cdot c = a \cdot (b \cdot c)$.

2. Identity: There exists an element $e \in G$, called the identity element, such that for all $a \in G, e \cdot a = a \cdot e = a$.

3. Inverse: For each $a \in G$,there exists an element $a^{-1} \in G$,called the inverse of a, such that $a \cdot a^{-}1 = a^{-1} \cdot a = e$.

Definition 6 A Lie group is a mathematical structure that combines the concepts of a group and a differentiable manifold. Specifically, a Lie group is defined as follows: A Lie group is a group G that is also a differentiable manifold, such that:

1. The group multiplication operation $\mu : G \times G \to G$, defined by $\mu(a, b) = ab$ for $a, b \in G$, is differentiable.

2. The group inversion operation $i : G \to G$, defined by $i(a) = a^{-1}$ for $a \in G$, is differentiable.

In other words, a Lie group is a smooth manifold equipped with a group structure where the group operations (multiplication and inversion) are smooth functions.

2.2.2 Tilde operator

The following operator will often be used in the following definitions to map a vector in $\mathbb{R}^n$ to a skew-symmetric matrix:

$$\sim: \mathbb{R}^n \to \mathbb{R}^{n \times n}$$
$$\begin{pmatrix} x_1 \\ x_2 \\ x_3 \end{pmatrix} \mapsto \begin{pmatrix} 0 & -x_3 & x_2 \\ x_3 & 0 & -x_1 \\ -x_2 & x_1 & 0 \end{pmatrix}$$

2.2.3 Special Orthogonal group SO(3)

Definition 7 The special orthogonal group SO(3) is a specific case of a Lie group. It represents the group of rotations in three-dimensional Euclidean space. SO(3) is the group of 3×3 orthogonal matrices with determinant +1. Formally:

$$SO(3) := \{R \in \mathbb{R}^{3\times3} \mid R^\top R = RR^\top = I_3, \det(R) = +1\}$$

Where R is the rotational matrix, $R^\top$ is the transpose of R, I_3 is the 3×3 identity matrix and $\det(R)$ is the determinant of R.

If R is a differentiable function of time, $\dot{R}R^\top$ and $R^\top\dot{R}$ are Skew-Symmetric and belonging to $\mathfrak{so}(3)$

$\mathfrak{so}(3) := \{\tilde{\omega} \in \mathbb{R}^{3\times3}; -\tilde{\omega} = \tilde{\omega}^\top\}$

2.2.4 Special Euclidean group SE(3)

Definition 8 SE(3) is the group of rigid body motions in three-dimensional Euclidean space, consisting of rotations and translations. It can be represented as:

$$SE(3) := \left\{ \begin{pmatrix} R & t \\ 0_{1\times3} & 1 \end{pmatrix} \mid R \in SO(3), t \in \mathbb{R}^3 \right\}$$

Where t is a 3×1 translation vector and $0_{1\times3}$ is a 1×3 zero vector.

We denote an element of this group by $H \in SE(3)$. H_b^a is a homogeneous transformation matrix which describes how Ψ_b changes with respect to Ψ_a and is given by:

$$H_b^a := \begin{pmatrix} R_b^a & p_b^a \\ 0 & 1 \end{pmatrix}, \tag{2.3}$$

where $p_b^a \in \mathbb{R}^3$ denotes the displacement vector.

Definition 9 The Lie algebra of SE(3), denoted as $\mathfrak{se}(3)$, is defined as:

$$\mathfrak{se}(3) := \left\{ \tilde{T} = \begin{bmatrix} \tilde{\omega} & v \\ 0 & 0 \end{bmatrix} \in \mathbb{R}^{4\times4} \mid T = \begin{bmatrix} \omega \\ v \end{bmatrix} \in \mathbb{R}^6 \right\}$$

Where T is called the Twist, representing the velocity of an object in 3D space, $\tilde{\omega} = \begin{bmatrix}\omega_x & \omega_y & \omega_z\end{bmatrix}^\top \in \mathbb{R}^{3\times 3}$ is the angular velocity and $v = \begin{bmatrix}v_x & v_y & v_z\end{bmatrix}^\top \in \mathbb{R}^3$ represents the translational velocity.

The Lie algebra $\mathfrak{se}(3)$ can be identified with $\mathbb{R}^6$ through the vector space isomorphism

$$\begin{aligned} &\sim: \mathbb{R}^6 \to \mathfrak{se}(3) \\ &T = \begin{pmatrix} \omega \\ v \end{pmatrix} \mapsto \begin{pmatrix} \tilde{\omega} & v \\ 0 & 0 \end{pmatrix} = \tilde{T} \end{aligned} \tag{2.4}$$

Exponential map which maps from the algebra $\mathfrak{se}(3)$ to the group SE(3) are denoted as:

$$\mathrm{Exp}_{\mathrm{SE(3)}} : \mathfrak{se}(3) \to SE(3) \tag{2.5}$$

Definition 10 The dual of the Lie algebra $\mathfrak{se}(3)$ is denoted by $\mathfrak{se}(3)^*$ and defined as:

$$\mathfrak{se}^*(3) := \left\{ \tilde{W} = \begin{bmatrix} \tilde{\tau} & F \\ 0 & 0 \end{bmatrix} \in \mathbb{R}^{4\times 4} \mid W = \begin{bmatrix} \tau \\ F \end{bmatrix} \in \mathbb{R}^6 \right\}$$

Where W is called the Wrench, representing the forces of an object in 3D space, $\tilde{\tau} = \begin{bmatrix}\tau_x & \tau_y & \tau_z\end{bmatrix}^\top \in \mathbb{R}^{3\times 3}$ is the torque and $F = \begin{bmatrix}F_x & F_y & F_z\end{bmatrix}^\top \in \mathbb{R}^3$ represents the dual of the translational velocity.

Likewise, the Lie algebra $\mathfrak{se}^*(3)$ can be identified with $\mathbb{R}^6$ through the vector space isomorphism

$$\begin{aligned} &\sim: \mathbb{R}^6 \to \mathfrak{se}^*(3) \\ &W = \begin{pmatrix} \tau \\ F \end{pmatrix} \mapsto \begin{pmatrix} \tilde{\tau} & F \\ 0 & 0 \end{pmatrix} = \tilde{W} \end{aligned} \tag{2.6}$$

2.2.5 Change of frames

Suppose we have two homogeneous transformation matrices H_b^a and H_c^b. Then, we can describe the change of Ψ_i with respect to Ψ_j through Ψ_k:

$$H_i^j = H_k^j H_i^k \tag{2.7}$$

The transformation of twists T and wrenches W between any two frames Ψ_j and Ψ_i is as follows:

$$T_k^{j,l} = Ad_{H_i^j} T_k^{i,l} \tag{2.8}$$

($T_k^{j,l}$: The Twist of Ψ_k, with respect to Ψ_l, expressed in Ψ_j).

$$(W_b^i) = Ad_{H_i^j}^\top (W_b^j) \tag{2.9}$$

(W_b^i: The wrench of Ψ_b, expressed in Ψ_i).

Where the map $Ad_{H_i^j} : \mathbb{R}^6 \to \mathbb{R}^6$ is the Adjoint matrix of $H_i^j \in SE(3)$, given by:

$$Ad_{H_i^j} := \begin{pmatrix} R_i^j & 0 \\ p_i^j R_i^j & R_i^j \end{pmatrix}. \tag{2.10}$$

2.2.6 Lie bracket

By the identity property of the Lie bracket $[X, Y] = X(Y) - Y(X)$, with X, Y being vector fields:

$$ad_{T_i^{j,k}} T_i^{j,k} = [T_i^{j,k}, T_i^{j,k}] = 0 \tag{2.11}$$

With $ad_{T_i^{j,k}}$ being the small adjoint operator defined as:

$$ad_{T_i^{j,k}} := \begin{pmatrix} \omega_i^{j,k} & 0 \\ v_i^{j,k} & \omega_i^{j,k} \end{pmatrix}. \tag{2.12}$$

3 Configuration space and Kinematics formulation

In this chapter, we formulate the kinematics of the Cosserat beam. We shall begin by defining the configuration space of the model and explain how the use of a principle bundle structure can help us to derive the model in an intrinsic way. Through this geometric structure, we formulate the kinematics and dynamics of the model. The interested reader is referred to [11], which explains in a mathematically rigorous way the formulation and benefits of such structure.

An interesting point is how we can describe the configuration space of the Cosserat beam. In some works, it is modeled as an infinite product space of Lie groups, whereas other authors use the structure of a principle bundle. On top of that, there are also be variations between authors on where they choose to start with their formulation as [12] and [13] start from the intrinsic material (body) manifold and map its material points to the Euclidean space $\mathcal{E}^3$, whereas other other authors start with a description of a parameterized curve already embedded in Euclidean space [**?**][14].

In the general context of nonlinear elasticity problems for the formulation of strain, [12] uses the base space in terms of deformations in the metric structure. Whereas [13] shows for a static equilibrium case, that such expression can also be achieved by measuring the infinitesimal change of the Maurer-Cartan form, which is a connection and requires less mathematical structure.

3.1 Defining the configuration space: geometric structures

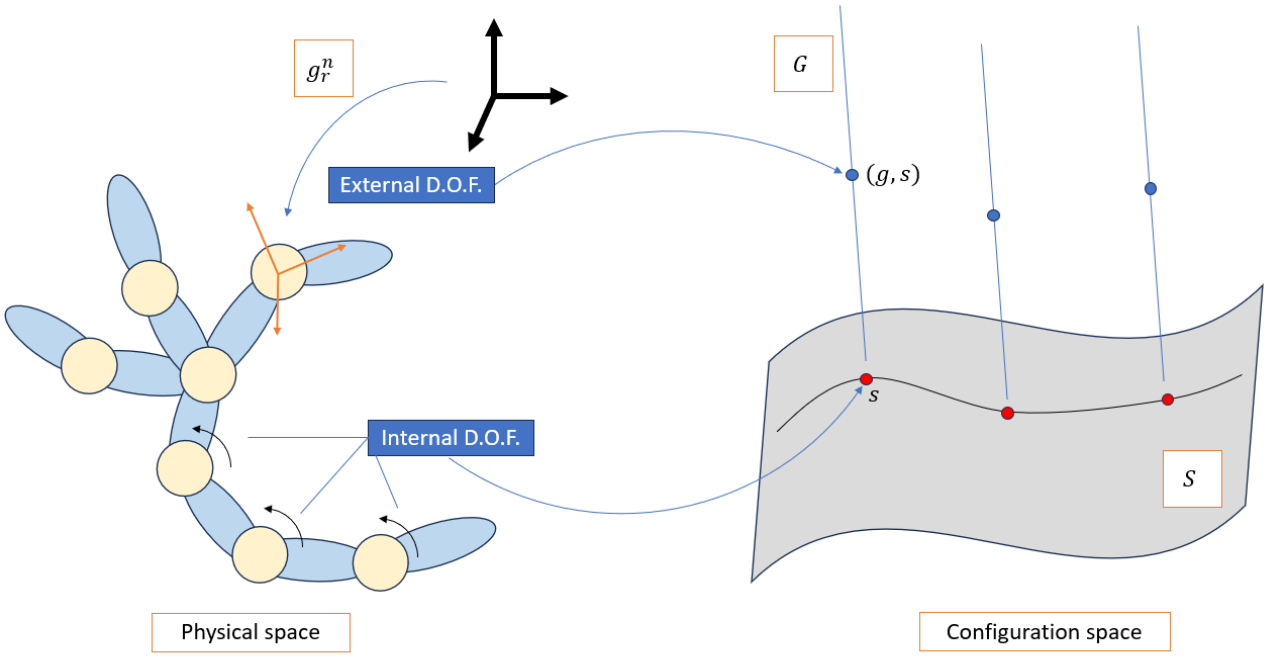

Figure 2: Visual interpretation of a principal bundle

A principal bundle is a fiber bundle with its fibers as Lie groups (denoted by G), and the base space (also called shape space) denoted by S. A visual representation is shown in Figure 2. Thus a point on the principle bundle is denoted by (g, s), with $s \in S$ and $g \in G$. This (trivial) principal bundle is then the configuration space (generally called the total space) $Q = G \times S$ of the model.

In the context of geometric mechanics, the principle bundle is a geometric structure which can be used in order to split the internal degrees of freedom (joints, deformations etc.) from the external degrees of freedom (a reference frame on one of the bodies; a floating frame or root frame)[15]. In that way, we are able to look at the model both in an intrinsic and extrinsic way.

The external degrees of freedom captures the "large" movements of the system with respect to an inertial frame Ψ_n, whereas the internal degrees of freedom captures the relative movements or deformations of the system. The external degrees of freedom are sometimes called "net" transformations.

The above is also called the "Floating frame" approach in [16], which is in contrast with the "Galilean" approach,

where each cross-section itself is referenced to an inertial frame and the configuration space can take the form of: $C = G \times G \times \cdots \times G$ when parameterized through Lie groups.

The elements of S and of the group G are related through a "connection". In other words, the (internal) shape velocities and the (external) net velocities are related by:

$$Ad_g\left(A(s)\dot{s}\right) = -Ad_g\left(\eta\right) \tag{3.1}$$

With $A(s) : T_gQ \to \mathfrak{g}$ being the "connection 1-form" and $\eta \in \mathfrak{g}$. A connection tells us the constraints that the fiber has with respect to the shape space. If the tangent vector in the configuration space is purely along the fibre, then the projection of the vector to the shape manifold is zero and would correspond to a purely rigid body motion of the system.

3.2 Kinematics

In accordance to this structure, we can write the kinematics for the Cosserat rod in the following way:

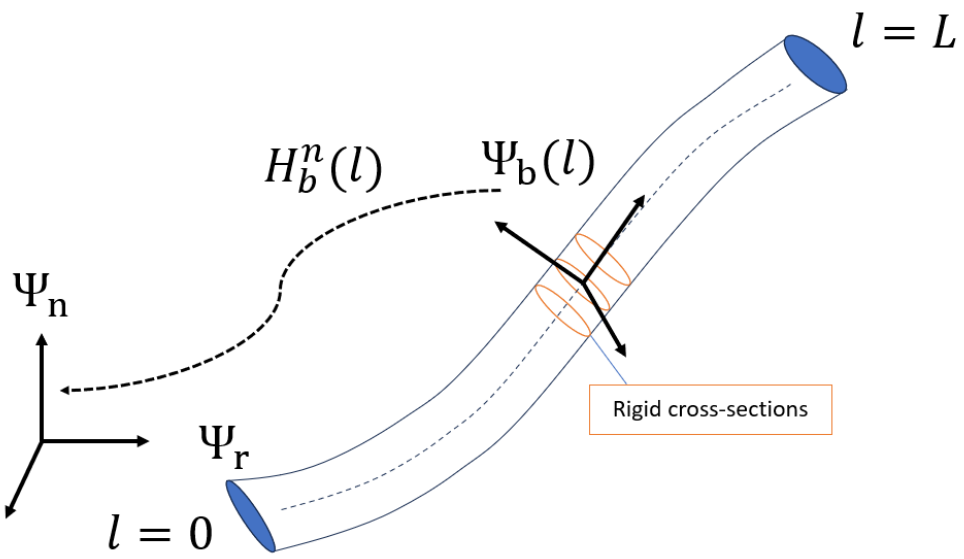

Figure 3: Model of the Cosserat rod

Split the rod $\mathcal{B}$ as shown in Figure 3 with length L up into infinitesimally small rigid cross-sections. These cross-sections have frames $\Psi_b(l)$ attached and are connected through a "backbone" curve parametrized by $l \in [0, L]$. On one particular cross-section $l(0)$ we call its frame the root frame. Let $H_b^n(0) = H_r^n \in \Omega^0(\mathcal{B}; SE(3))$ be the homogeneous transformation matrix which represents the (external) net transformations of the cross-sectional body root frame Ψ_r with respect to the inertial frame Ψ_n.

$$H_r^n = \begin{pmatrix} R_r^n & p_r^n \\ 0 & 1 \end{pmatrix} \tag{3.2}$$

where $R_r^n \in \mathbb{R}^{3\times3}$ and $p_r^n \in \mathbb{R}^3$ respectively denote the rotational and the translational components of the transformation.

Then a local transformation $H_r^b(l) \in \Omega^0(\mathcal{B}; SE(3))$ of a cross-section $\Psi_b(l)$ with respect to the root frame is given by:

$$H_{b(l)}^r = H_b^r(l) = \begin{pmatrix} R_b^r(l) & p_b^r(l) \\ 0 & 1 \end{pmatrix} \tag{3.3}$$

Then according to Equation 2.7, we can also express the change of the body frame Ψ_b with respect to the inertial frame Ψ_n:

$$H_b^n(l) = H_r^n H_b^r(l) \tag{3.4}$$

Denote $H \in \Omega^0(\mathcal{B}; SE(3))$ as the field of local homogeneous transformations over the beam.

A local strain $\tilde{\xi}_b^{b,r}(l) \in \Omega^0(\mathcal{B}; se(3))$ is defined as:

$$\tilde{\xi}_b^{b,r}(l) := H_r^b(l)^{-1} H_r^b(l)' \tag{3.5}$$

Note that we often interchange an element of the Lie group $\tilde{\xi}_b^{b,r}(l)$ with $\xi_b^{b,r}(l) \in \mathbb{R}^6$ through its isomorphism.

Let a point $(H_r^n, \tilde{\xi})$ represent one configuration of the rod in terms of the root frame and the local body strain of all slices defined as the strain field $\tilde{\xi} \in \Omega^0(\mathcal{B}; se(3)) =: \tilde{S}$. Then the configuration space is defined as:

$$\begin{aligned} \tilde{Q} &= SE(3) \times \tilde{S} \\ (H_r^n, \tilde{\xi}) &\in \tilde{Q} \end{aligned} \tag{3.6}$$

In case of a continuum model, the point on $\tilde{Q}$ contain an infinite amount of strains since each of the slices are modelled infinitesimally. We will see later how this can be reduced to a finite dimensional space in order for it to be used for simulation.

By knowing the root frame transformation H_r^n and integrating the (material) strain twist over the domain l, we can reconstruct the configuration of the rod.

However, since the local strain is not constant (it has a dependency on l), it cannot simply be evaluated as with an ordinary differential equation with constant values. As such, one can approximate the solution of Equation 3.5 through the Magnus expansion [17].

Let a curve γ be parameterized by time $t \in \mathbb{R}$. Then $\gamma(t)$ on $\tilde{Q}$ represents the change of configuration over time t. By this, the homogeneous transformation H_b^n and H_r^b becomes next to its spacial dependency, also time-dependent and thus we introduce next to the local strain also a local velocity:

$$\tilde{T}_b^{b,r}(l,t) = H_r^b(l,t)^{-1}\dot{H}_r^b(l,t) \tag{3.7}$$

With again the isomorphism between the velocity Twist vector $T_b^{b,r} \in \mathbb{R}^6$ and the Lie algebra element $\tilde{T}_b^{b,r} \in se(3)$. The collection of the local velocity twists of all slices are denoted by $\tilde{T} \in \Omega^0\left(\mathcal{B}; se(3)\right)$.

The compatibility equation relates the strain-rate with the spacial twist is given as follows. Due to equality of mixed partials:

$$\frac{\partial}{\partial t}\left(\frac{\partial H}{\partial l}\right) = \frac{\partial}{\partial l}\left(\frac{\partial H}{\partial t}\right) \tag{3.8}$$

Substituting Equation 3.5 and Equation 3.7 and applying chain rule gives:

$$H\tilde{T}\tilde{\xi} + H\frac{\partial \tilde{\xi}}{\partial t} = H\tilde{\xi}\tilde{T} + H\frac{\partial \tilde{T}}{\partial l} \tag{3.9}$$

Then by multiplying with the inverse of H we get:

$$\frac{\partial \tilde{T}}{\partial l} = -\left(\tilde{\xi}\tilde{T} - \tilde{T}\tilde{\xi}\right) + \frac{\partial \tilde{\xi}}{\partial t} \tag{3.10}$$

In which we recognize the Lie bracket term (Equation 2.11):

$$\tilde{\xi}\tilde{T} - \tilde{T}\tilde{\xi} = ad_{\tilde{\xi}}\tilde{T} \in \Omega^0\left(\mathcal{B}; se(3)\right) \tag{3.11}$$

And due to the tilde isomorphism results in:

$$\xi T - T\xi = ad_{\xi}T \in \Omega^0\left(\mathcal{B}; \mathbb{R}^6\right) \tag{3.12}$$

Then Equation 3.10 results in:

$$T' = \dot{\xi} - \mathrm{ad}_{\xi}T \in \Omega^0\left(\mathcal{B}; \mathbb{R}^6\right) \tag{3.13}$$

Finally, taking the time-derivative of Equation 3.13 (and applying the product rule on the term with the adjoint) gives

$$\dot{T}' = \ddot{\xi} - \mathrm{ad}_{\dot{\xi}}T - \mathrm{ad}_{\xi}\dot{T} \in \Omega^0\left(\mathcal{B}; \mathbb{R}^6\right) \tag{3.14}$$

3.3 Reconstruction of geometry: The Magnus Expansion

In order to reconstruct a configuration of the rod, we need to integrate Equation 3.5. However, this is not as trivial since we are not dealing with simple scalar differential equations but with elements in the $SE(3)$ group instead.

Consider as an example the following scalar linear differential equation:

$$\dot{y} = y \cdot a(t) \in \mathbb{R}, \quad y(0) = y_0, t \geq 0 \tag{3.15}$$

This will have the solution:

$$y(t) = y_0 \cdot \exp\left(\int_0^t a(s)ds\right) \in \mathbb{R} \tag{3.16}$$

This is not always true in the case of differential equations in matrix form:

$$\dot{Y} = YA(t) \in \mathbb{R}^{n\times n}, \quad Y(0) = Y_0, t \geq 0 \tag{3.17}$$

The only case that Equation 3.17 would be having a solution structure of the form as shown in Equation 3.15, would be when $A(t_1)$ and $A(t_2)$ commute. In other words, when:

$$[A(t_1), A(t_2)] = 0 \rightarrow A(t_1)A(t_2) = A(t_2)A(t_1), \quad \forall t_1, t_2 \geq 0. \tag{3.18}$$

From Equation 3.18, this would clearly be the case for a constant matrix A.

Now, recall Equation 3.5 is written in the form $\dot{Y} = YA(t)$. A solution in the form of Equation 3.16 would be desirable, since if Y is an element of the Lie group and A is an element in its algebra, it would give us a solution that is an element of the group through the exponential mapping (as stated in the preliminaries).

One way to achieve this is through the use of the Magnus series $\widetilde{\Omega}(l) \in se(3)$ [17][18]:

$$H_b^n(l) = H_r^n \exp\left(\widetilde{\Omega}(l)\right), \tag{3.19}$$

Note that H_r^n is the initial condition.

In case for a constant strain ($\xi(l) = \xi$), the expansion would lead to the following:

$$\widetilde{\Omega}(l) = \int_0^l \tilde{\xi} ds \tag{3.20}$$

The actual computation of $\widetilde{\Omega}(l)$ for non-constant strain involves the approximation of $\widetilde{\Omega}(l)$ and will be discussed in chapter 7.

3.4 Conclusion

In this chapter the kinematics have been defined by a strain parametrization approach. We have seen that the configuration space comes in the form of a principle bundle structure which separates the internal degrees of freedom (local strains) from the external degrees of freedom. To retrieve a configuration of the rod through the strain, we noted that we need the Magnus expansion to evaluate Equation 3.5.

4 Dynamics

4.1 Hamilton's Principle of least action

There are multiple derivations for the dynamics for the Cosserat beam model found in literature. Often the three main derivations found are applying the variational principle on either the Newton-Euler equations, the Hamiltonian or the Lagrangian. In this section, we will derive the dynamics of the Cosserat beam through the Lagrangian in order to show that the energy is conserved.

We follow the steps from [19] and begin by stating the Hamiltonian principle of least action:

$$\int_{t1}^{t2} \delta L dt = 0 \tag{4.1}$$

The action is defined as the time integral of the Lagrangian function L and a variation (of the action) is denoted by δ (which informally can be seen as a small change of the Lagrangian function).

Broadly speaking, action is a scalar quantity that describes the evolution of a system's kinetic and potential energy balance along its trajectory. The least action principle minimizes the action. This is true when the variational terms are equal to zero, as stated in Equation 4.1

Since we are dealing with a system of infinitesimal rigid bodies, the Lagrangian is described by a Lagrangian density function and the equation becomes:

$$\int_{t1}^{t2} \delta \int_{0}^{L} \mathcal{L} dl dt = 0 \tag{4.2}$$

Where the Lagrangian density function $\mathcal{L} : SE(3) \times TSE(3) \times TSE(3) \to \mathbb{R}$ is a function of the transformations of the cross-sections and their spatial and time derivatives:

$$\mathcal{L}\left(H_r^b(l), H_r^b(l)', \dot{H}_r^b(l)\right)$$

And since the field representations of Equation 3.5 and Equation 3.7 states that:

$$\tilde{T} = H^{-1}\dot{H}(l) \in \Omega^0(\mathcal{B}; se(3))$$
$$\tilde{\xi} = H^{-1}H'(l) \in \Omega^0(\mathcal{B}; se(3))$$

We can rewrite the variables $H', \dot{H} \in TSE(3)$ of $\mathcal{L}$ as the variables $T, \xi \in \mathbb{R}^6$ respectively. This is the so-called 'reduced' Lagrangian density function $\mathcal{L} : SE(3) \times \mathbb{R}^6 \to \mathbb{R}$, since now the derivatives do not depend explicitly on H.

$$\begin{aligned} L &= \int_0^L \mathcal{L}(H, H', \dot{H}) dl \\ &= \int_0^L \mathcal{L}(H, T, \xi) dl \end{aligned} \tag{4.3}$$

We note that the δ operator is commutative; the time and space variations can therefore be written as:

$$\delta(\dot{H}) = (\delta\dot{H}) \tag{4.4}$$
$$\delta(H') = (\delta H)' \tag{4.5}$$

Define the field material variation of H as:

$$\delta\tilde{\zeta} = H^{-1}\delta H \in \Omega^0(\mathcal{B}; se(3)) \tag{4.6}$$

Then substituting $\delta H = H\delta\tilde{\zeta}$ into Equation 4.5 gives the following relations through the Poincaré equations [19] (See appendix [A] for the proof):

$$\delta T = (\dot{\delta\zeta}) + ad_T(\delta\zeta) \in \Omega^0(\mathcal{B}; \mathbb{R}^6), \tag{4.7}$$

$$\delta\xi = (\delta\zeta)' + ad_\xi(\delta\zeta) \in \Omega^0(\mathcal{B}; \mathbb{R}^6) \tag{4.8}$$

Which makes it possible to apply variational calculus using Lie groups.

4.2 Equations of motion

The variation of the Lagrangian function is then defined as:

$$\int_{t1}^{t2} \delta L = \int_{t1}^{t2} (\delta \mathcal{K} + \delta \mathcal{U}_{int} - \delta \mathcal{U}_{ext})\, dt \tag{4.9}$$

With $\mathcal{K}$ as the total kinetic energy of the beam and $\mathcal{U}_{int}$ and $\mathcal{U}_{ext}$ as the internal strain and external energy of the beam respectively.

4.2.1 Kinetic energy

The kinetic energy function is defined as:

$$\mathcal{K} = \frac{1}{2} \int_0^L \left((T_b^{b,r})^\top \mathcal{I} T_b^{b,r} \right) \tag{4.10}$$

The variation of the kinetic energy function is then found by applying the product rule on Equation 4.10:

$$\begin{aligned} \delta \mathcal{K} &= \int_0^L \frac{1}{2} \left(\delta (T_b^{b,r})^\top \mathcal{I} T_b^{b,r} + (T_b^{b,r})^\top \mathcal{I} \delta T_b^{b,r} \right) dl \\ &= \int_0^L \delta (T_b^{b,r})^\top \mathcal{I} T_b^{b,r} dl \end{aligned} \tag{4.11}$$

Where $\mathcal{I} : se(3) \times se(3) \to \mathbb{R}$ is the 6×6 mass density tensor.

Following from Equation 4.7, the expression of $\delta(T_b^{b,r})$ is given as:

$$\delta T = (\dot{\delta \zeta}) + ad_T(\delta \zeta)$$

Inserting Equation 4.7 into Equation 4.12 and integrate it with respect to time:

$$\int_{t1}^{t2} \delta \mathcal{K} = \int_{t1}^{t2} \int_0^L \left((\dot{\delta \zeta})^\top \mathcal{I} T + ad_T(\delta \zeta)^\top \mathcal{I} T \right) dl dt \tag{4.12}$$

The goal is to factor out the $\delta\zeta$. This is done by applying integration by parts on the first term in the right side, containing the $\dot{\delta\zeta}$ (Equation 4.13):

$$\int_{t1}^{t2} \delta \mathcal{K} = \int_{t1}^{t2} \int_0^L \left((\dot{\delta \zeta})^\top \mathcal{I} T \right) dl dt + \int_{t1}^{t2} \int_0^L \left(ad_T(\delta \zeta)^\top \mathcal{I} T \right) dl dt \tag{4.13}$$

Assuming the mass density matrix is time independent:

$$\int_{t1}^{t2} \int_0^L \left((\dot{\delta \zeta})^\top \mathcal{I} T \right) dl dt = \left[\int_0^L \delta \zeta^\top \mathcal{I} T dl \right]_{t1}^{t2} - \int_{t1}^{t2} \int_0^L \left((\delta \zeta)^\top \mathcal{I} \dot{T} \right) dl dt \tag{4.14}$$

Substituting Equation 4.14 into Equation 4.13 leads to the weak form of the kinetic energy:

$$\int_{t1}^{t2} \delta \mathcal{K} dt = \left[\int_0^L \delta \zeta^\top \mathcal{I} T dl \right]_{t1}^{t2} - \int_{t1}^{t2} \int_0^L \delta \zeta^\top (\mathcal{I} \dot{T} - ad_T^\top \mathcal{I} T) dl dt \tag{4.15}$$

With the first term on the right side being zero due to the variations being fixed at the boundaries.

4.2.2 Strain energy

The internal strain energy of the beam is defined as:

$$\mathcal{U}_{int} = \frac{1}{2} \int_0^L \xi^\top r dl \tag{4.16}$$

Where r is defined as the stress resultant vector over a cross-section of the beam.

Using a simple stress-strain relation:

$$r = E\xi \tag{4.17}$$

With $E : se(3) \times se(3) \to \mathbb{R}$ being the 6×6 stiffness density tensor.

Taking the variation of the internal energy (Equation 4.16) gives:

$$\begin{aligned}\delta(\mathcal{U}_{int}) &= \int_0^L \frac{1}{2}\left(\delta(\xi)^\top E\xi + \xi^\top E\delta(\xi)\right) dl \\ &= \int_0^L \left(\delta(\xi)^\top E\xi\right) dl\end{aligned} \tag{4.18}$$

Recall that an expression for $\delta\xi$ is stated in Equation 4.8:

$$\delta\xi = (\delta\zeta)' + ad_\xi(\delta\zeta) \tag{4.19}$$

Like in the case for the kinetic energy above, the goal is to pull out the $\delta\zeta$ factor out. Substituting Equation 4.8 into Equation 4.19 and integrating by parts with respect to the material instead of the time domain leads to the weak form of the internal energy:

$$\int_{t1}^{t2} \delta(\mathcal{U}_{int})dt = \left[\int_{t1}^{t2} \delta\zeta^\top E\xi dt\right]_0^L - \int_{t1}^{t2}\int_0^L \delta\zeta^\top \left(E\xi' - ad_\xi^\top E\xi\right) dldt \tag{4.20}$$

With the first term on the right side being considered the boundary conditions.

4.2.3 External energy

The external energy consist of the gravitational forces on the cross-sections of the beam and is given as:

$$\mathcal{U}_{ext} = \delta\zeta(0)^\top \mathbf{g}(0) - \delta\zeta(L)^\top \mathbf{g}(L) - \int_0^L \delta\zeta^\top \mathbf{g}(l)dl \tag{4.21}$$

With $\mathbf{g}(l)$ being the gravitational force on the cross-section:

$$\mathbf{g}(l) = \begin{bmatrix} mgR(l)^\top e \\ 0_{3\times 1}\end{bmatrix} \tag{4.22}$$

With $e = \begin{bmatrix}0 & 0 & 1\end{bmatrix}^\top$ is the unit vector in the z-direction, g being the gravitational constant and m is the mass density of the cross-section.

The time integral of the variation of the external energy comes from the gravitational forces and can be expressed as:

$$\int_{t1}^{t2} \delta(\mathcal{U}_{ext}) = \int_{t1}^{t2} \left[\delta\zeta^\top \mathbf{g}\right]_0^L dt - \int_{t1}^{t2}\int_0^L \delta\zeta^\top \mathbf{g} dldt \tag{4.23}$$

4.2.4 Variational- and strong form

Inserting the found variational expressions for the kinetic (Equation 4.14) and internal and external energies (Equation 4.20 & Equation 4.23) into the least action principle Equation 4.9 we obtain the weak form of the equations of motion:

$$[\delta\zeta^\top(E\xi - \mathbf{g})]_0^L - \int_0^L \delta\zeta^\top(-\mathcal{I}\dot{T} + ad_T^\top \mathcal{I}T + E\xi' - ad_\xi^\top E\xi + \mathbf{g})dl = 0, \quad \forall\delta\zeta \tag{4.24}$$

If we realize this should hold for all possible $\delta\zeta$, we obtain the strong form of the partial differential equation for the dynamics of a cosserat beam by again applying ('reverse') integration by parts:

$$\mathcal{I}\dot{T} - ad_T^\top \mathcal{I}T - E\xi' + ad_\xi^\top E\xi = \mathbf{g} \in \Omega^0(\mathcal{B};\mathbb{R}^6) \tag{4.25}$$

Where we notice that Equation 4.25 are the components of the volume form $dl \in \Omega^1(\mathcal{B};\mathbb{R})$

Overall, the total equations of motion are:

- Kinematics

$$\begin{aligned} H' &= H\tilde{\xi} \\ T' &= \dot{\xi} - \mathrm{ad}_{\xi} T \\ \dot{T}' &= \ddot{\xi} - \mathrm{ad}_{\dot{\xi}} T - \mathrm{ad}_{\xi} \dot{T} \end{aligned}$$

- Boundary conditions

$$[E\xi(l) - \mathbf{g}]_0^L$$

- Dynamics

$$\mathcal{I}\dot{T} - ad_T^\top \mathcal{I} T - E\xi' + ad_\xi^\top E\xi = \mathbf{g}$$

4.3 Conservation of energy: Continuous

The overall energy balance for the continuous system is written as:

$$\mathcal{K} + \mathcal{U}_{int} = \mathcal{U}_{ext} \tag{4.26}$$

With the kinetic, internal- and external energies given resp. in Equation 4.10, Equation 4.16 and Equation 4.21.

4.4 conclusion

In this chapter, we have derived the dynamics of the Cosserat rod and thus fully defined its equations of motion. By using the Lagrangian approach, we can conclude that the system in the continuous case abides by the energy laws.

5 Model reduction

5.1 Reduced Kinematics

In this chapter, we closely follow the work of [20]. Suppose that the strain field $\xi = [\xi_1, \xi_2, ..., \xi_6] \in \Omega^0\left(\mathcal{B}; \mathbb{R}^6\right)$ can be expressed as an infinite series of spatially varying basis functions and their corresponding time-dependent coefficients. Then, a component i of the strain field can be written as:

$$\xi_i(l,t) = \sum_{n=1}^{k=\infty} \theta_n(l) q_{i,n}(t) + \xi_i^\circ(l) \quad i \in \{1, \dots, 6\} \tag{5.1}$$

With coefficient $q_{i,n}(t)$ and a time-invariant strain $\xi_i^\circ(l)$. In general, one can choose any set of basis functions as long as they are orthogonal to one another $\left(\int_0^L \theta_i(l)\theta_j(l)dl = 0\right)$. This orthogonality property means that one basis functions cannot be expressed as a sum of other basis functions, making the solution of how the field components can be described unique.

Due to this rewriting of the strain field, the base space S of the principle bundle changes from $\Omega^0(\mathcal{B}; se(3))$ to $\Omega^0(\mathcal{B}; \mathbb{R}^k)$. Now uniqueness is guaranteed but the problem of computation remains when $k = \infty$. This is why we approximate the original strain field with a truncated strain field $[\xi]_k$, with $k < \infty$.

The above can also be written more compactly in its vector formulation, with the truncated strain field $[\xi]_k$.

$$[\xi]_k(l,t) = \Phi(l)q(t) + \xi_o(l), \quad k < \infty. \tag{5.2}$$

with $\Phi \in \mathbb{R}^{6\times 6k}$.

Taking the derivative of Equation 5.3 with respect to time gives:

$$[\dot{\xi}]_k(l,t) = \Phi(l)\dot{q}(t), \quad k < \infty. \tag{5.3}$$

We would also like to express the rest of the kinematic equations in terms of the truncated strain field. Recall that the twist is $T' = \dot{\xi} - \mathrm{ad}_\xi T$ and we want to integrate this expression to find the velocity twist field T. We do this by using the differential property of the adjoint action

$$ad_\xi = -\frac{\partial}{\partial l}[Ad_{H^{-1}}]Ad_H \tag{5.4}$$

so that Equation 3.13 of the twist becomes:

$$T' = \dot{\xi} + \frac{\partial}{\partial l}[Ad_{H^{-1}}]Ad_H T \tag{5.5}$$

$$= \Phi(l)\dot{q}(t) + \frac{\partial}{\partial l}[Ad_{H^{-1}}]Ad_H T \tag{5.6}$$

It can be shown in [20] that integrating Equation 5.6 gives:

$$[T]_k(l, q, \dot{q}) = {Ad_{[H]_k}}^{-1} \left(\int_0^l Ad_{[H]_k}\Phi(l)ds \right) \dot{q} \tag{5.7}$$

Writing the geometric Jacobian in Equation 5.8 as:

$$[J]_k := Ad^{-1}_{[H]_k(L,q)} \int_0^l Ad_{[H]_k(s,q)}\Phi(l)ds \quad \in \mathbb{R}^6 \times \mathbb{R}^{6k} \tag{5.8}$$

We can rewrite the twist as Equation 5.9 in its compact form:

$$[T]_k = [J]_k\dot{q} \tag{5.9}$$

Finally, for the acceleration term we take the time derivative of the above:

$$[\dot{T}]_k = [J]_k\ddot{q} + [\dot{J}]_k\dot{q} \tag{5.10}$$

Again, by referring to [20] the time derivative of Equation 5.8 is given as:

$$[\dot{J}]_k = Ad^{-1}_{[H]_k} \int_0^L Ad_{H_k} ad_{[T]_k}\Phi ds \tag{5.11}$$

5.2 Reduced Dynamics

In order to make the obtained reduced order kinematics usable for formulating the dynamics, we first need to also project the Mass and stiffness matrices onto the generalized coordinates through the geometric Jacobian:

$$M(q) = \int_0^L [J]_k^\top \mathcal{I} [J]_k dl \in \mathbb{R}^{k \times k}, \tag{5.12}$$

$$K(q) = \int_0^L [J]_k^\top E [J]_k dl \in \mathbb{R}^{k \times k}, \tag{5.13}$$

$$C(q, \dot{q}) = \int_0^L [J]_k^\top \left(\mathcal{I} [\dot{J}]_k + \mathcal{C}_{[T]_k} [J]_k \right) dl \in \mathbb{R}^{k \times k}, \tag{5.14}$$

$$F = \int_0^L [J]_k^\top \mathbf{g} dl \in \mathbb{R}^k \tag{5.15}$$

With $\mathcal{C}_{[T]_k} := \mathcal{I} ad_{[T]_k} - ad_{[T]_k}^\top \mathcal{I}$.

By substituting Equation 5.9 and Equation 5.10 into the dynamics equation (Equation 4.26) we get the following reduced order dynamics:

$$M\ddot{q} + C\dot{q} + Kq = F \in \mathbb{R}^k \tag{5.16}$$

5.3 Reduced energy balance

As for the continuous case, the energy balance is given as a sum of the kinetic, elastic and gravitational potential energies:

$$\frac{1}{2} \dot{q}^\top M \dot{q} + \frac{1}{2} q^\top K q = M g z(q) \tag{5.17}$$

Where $z(q)$ is the z-component of the homogeneous transformation matrix H

5.4 Conclusion

We have projected the kinematics and dynamic equations from the previous chapter onto a set of orthogonal bases functions with their coefficients.

5.5 Choosing base functions

So far, it has not yet been decided what the bases functions from Equation 5.3 should look like. There are two kinds of bases functions to choose from: local bases functions or global bases functions. Where global base functions span over the entire domain of the rod, local base functions only have impact on certain subdomains of the rod.

5.5.1 Global bases

Global bases are constructed using global shape functions. These shape functions span over the entire domain of the beam. An example of a polynomial bases set can be seen in Figure 4, in which the first five Chebyshev polynomials are shown.

Figure 4: Chebyshev polynomials of the first kind

5.5.2 Local bases

Local bases are constructed using local polynomial shape functions. Normally, these shape functions are used for formulating the position field. In this case, they are used to model the strain field instead. Figure 5 shows an example of local shape functions.

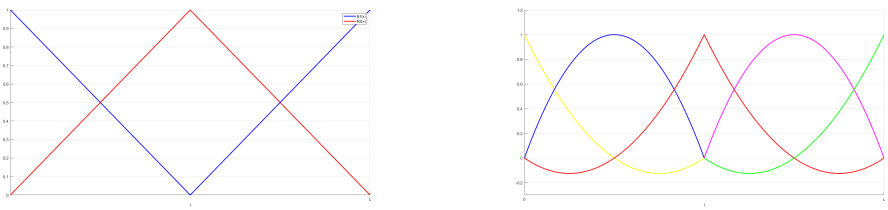

(a) Hat (b) Quadratic

Figure 5: Linear, quadratic and cubic shape functions

For the hat functions, the degrees of freedom are simply the outer nodal points of the element. However, for higher order polynomials, more nodal points (and thus more degrees of freedom) are needed for an element. This results in higher computation time but better accuracy. Due to the locality characteristics, a FEM-like bases shows better results when there is a point force applied to a part of the rod [21].

6 Discretization

So far, we have obtained the reduced equations of motion. However, these terms still involve techniques (like integration) which belong to the continuous domain. In this section we will explain how to approximate integrals in a discretized way and how the Magnus series can be approximated.

6.1 Gauss Quadrature

There are many numerical integration schemes (e.g. trapezoidal rule or Simpson's rule) available in order to evaluate the integrals which show up in the previous chapter. In this case, the integrals are approximated through the Gauss quadrature rule. The Gaussian quadrature approximation is given in Equation 6.1 as:

$$\int_a^b W(x)f(x)dx \approx \sum_{i=1}^{n} W_i f(x_i) \tag{6.1}$$

With $W(x)$ being a so-called "weight function", W_i being the "weights" and x_i being the nodes at which the values are computed. There are different variants of this Gaussian quadrature method with each their different weight functions. The Legendre-Gauss variant (Equation 6.2) which has a weight function of $W(x) = 1$, is the most used or general purposed variant for evaluating polynomial functions due to it being possible of calculating the integrals exactly provided that enough quadrature points are chosen. And since we are dealing with a strain parameterized approach with the strain field projected onto a set of polynomial functions (recall Equation 5.3), this would be a valid variant to choose.

$$\int_{-1}^{1} f(x)dx \approx \sum_{i=1}^{n} W_i f(x_i) \tag{6.2}$$

Note though that in this case, the integral goes over the domain $[-1, 1]$ while in our case most of the integrals goes from 0 (start of the rod) to L (end of the rod). It can however be generalized for an interval $[a, b]$ by a change of coordinates of the differential [22] which is shown as follows:

$$\int_a^b f(x)\ dx = \int_{-1}^{1} f\left(\frac{b-a}{2}(z) + \frac{a+b}{2}\right)\frac{b-a}{2}dz \tag{6.3}$$

This then results in:

$$\int_a^b f(x)dx \approx \frac{b-a}{2}\sum_{i=1}^{n} W_i f\left(\frac{b-a}{2}z + \frac{a+b}{2}\right) \tag{6.4}$$

In the case of the Cosserat rod, the components of Equation 5.16 can be calculated numerically as:

$$M(q) \approx \sum_{i=1}^{n} W_i [J]_k^\top \mathcal{I} [J]_k, \tag{6.5}$$

$$K(q) \approx \sum_{i=1}^{n} W_i [J]_k^\top E [J]_k, \tag{6.6}$$

$$C(q, \dot{q}) \approx \sum_{i=1}^{n} W_i [J]_k^\top \left(\mathcal{M}[\dot{J}]_k + \mathcal{C}_{[T]_k}[J]_k\right), \tag{6.7}$$

$$F \approx \sum_{i=1}^{n} W_i [J]_k^\top \mathbf{g} \tag{6.8}$$

And the Jacobian:

$$[J]_k \approx Ad^{-1}_{[H]_k(L,q)} \sum_{i=1}^{n} W_i Ad_{[H]_k(s,q)} \Phi(l) \tag{6.9}$$

6.2 Domain discretization and Magnus expansion

In order to compute the Magnus series, we follow the theory stated in [23].

First of all, like the Taylor series, the Magnus series will degrade when its taken over a large domain l of the Cosserat rod. In order to address this, the rod is divided into smaller intervals of length h_j and the homogeneous transformation matrices, Jacobians and its derivatives are then computed at the Gaussian quadrature points j shown as black dots in Figure 6:

$$H\big(l+h_j\big) = H(l)\exp\big(\widetilde{\Omega}(h_j)\big), \quad \sum_{0}^{j} h_j = L. \tag{6.10}$$

And $H(0) = I_{4\times 4}$.

It is shown in [24] that the maximum step size h can be:

$$h_{max} < \frac{\pi}{\sqrt{6\beta^2+1}} \tag{6.11}$$

With $\beta \in \mathbb{R}$ depending on the strain limit of the rod's material.

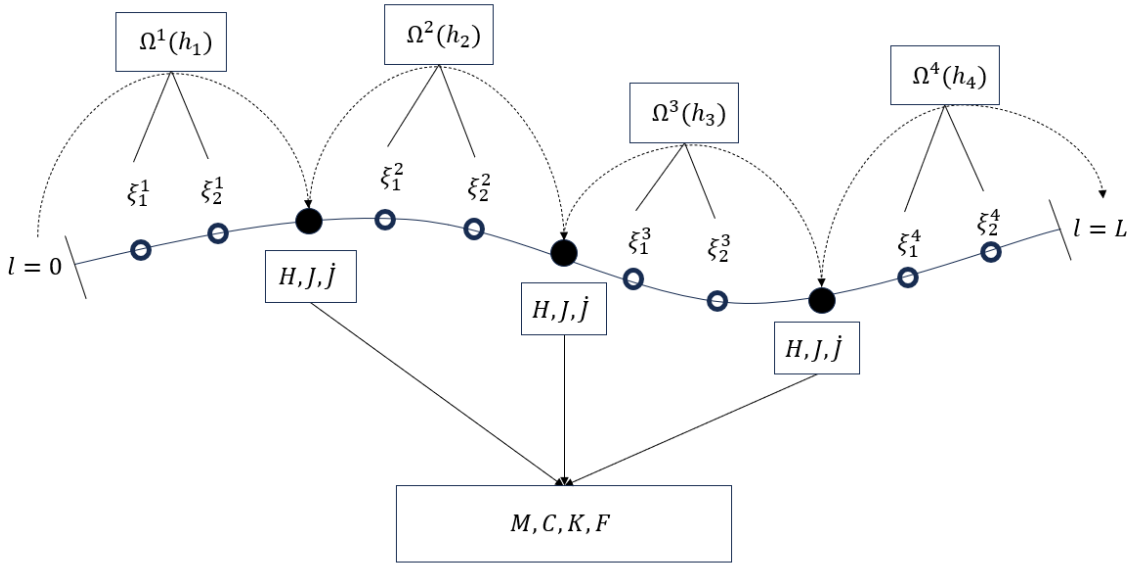

Figure 6: Example of a 4th order Zanna approximation with 3 Gauss quadrature points

The Magnus series $\widetilde{\Omega}$ can be approximated through the Zanna approximation method [25]. For instance, a fourth-order Zanna with two-stage Gauss quadrature is shown in figure Figure 6, which needs two values of the strain between two Gaussian quadrature points:

$$\Omega(h^j) = \frac{h_j}{2}(\xi_1^k + \xi_2^k) + \frac{\sqrt{3}h_j^2}{12}\mathrm{ad}_{\xi_1^k}\xi_2^k, \tag{6.12}$$

With $\tilde{\xi_1^k} = \tilde{\xi}\left(l + h_j/2 - \sqrt{3}h_j/6\right)$ and $\tilde{\xi_2^k} = \tilde{\xi}\left(l + h_j/2 + \sqrt{3}h_j/6\right)$ which are at the points in Figure 6 denoted by the open dots.

This is in contradiction to the statement in [10], where only the first term of the Magnus expansion is considered over the entire domain of the rod. This is problematic since this would only hold if the matrix expression is not dependent on spatial variable [17].

7 Coding & Implementation

In order to see the impact of the Magnus expansion, the SoRoSim toolbox has been used[23]. Sorosim is a Matlab toolbox that uses the Geometric Variable Strain (GVS) approach to provide a unified framework for the modeling, analysis, and control of soft, rigid, and hybrid robots. An overview of the SoRoSim algorithm is shown in Figure 7.

7.1 Computation algorithm

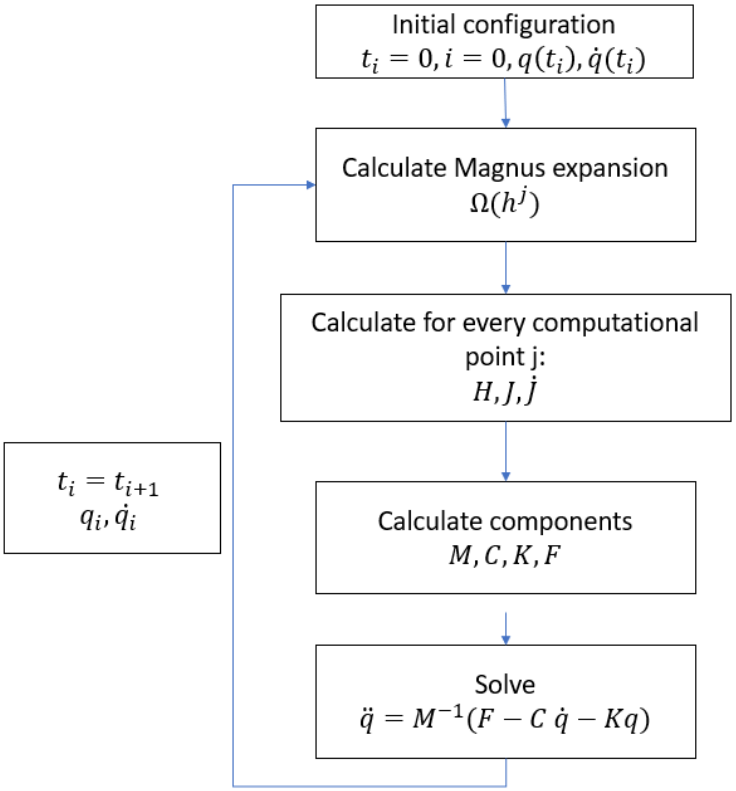

Figure 7: Computation scheme

The algorithm goes through the following steps:

1. At the start of the simulation when $t = 0$, initial conditions are given to q and $\dot{q}$. In our case, these will be equal to zero, meaning that the simulation starts with no initial velocity or displacement.

2. By knowing the initial conditions, the strain can be calculated through bases functions as shown in Equation 5.3.

3. Strains at certain points (the open dots in Figure 6) are then used in order to approximate the Magnus series (Equation 6.12).

4. Then H, J and $\dot{J}$ can be computed at those quadrature points and the components of Equation 5.16 are calculated.

5. After this, $\ddot{q}$ is calculated and through the ODE45 of Matlab [26] we retrieve q and $\dot{q}$ for the next time step. We then go through step 3 to step 5 again until the simulation time horizon has been reached.

7.2 Parameters

The following parameters are shared through all the executed simulation cases (Table 1).

Boundary conditions:	Fixed-Free
Profile:	Circular
Material density:	1000 $\frac{kg}{m^3}$
Youngs Modulus	1 $\cdot 10^6 \frac{N}{m^2}$
Material damping	0
Length	0.3 m
Radius	0.03 m
Gravity	-9.81 $\frac{m}{s^2}$
Active Strain modes	6
Initial values q	0
Initial values $\dot{q}$	0
ODE type	ODE45
Timestep	0.01

Table 1: Overview of the parameters used for simulation

8 Simulation results

During the use of the SoRoSim toolbox (version 6.3), it was noted that the elastic strain energy was faulty calculated Figure 8. Attempts were made to fix this issue, yet a proper solution still needs to be found in order for it to produce results with machine precision on its own. For now, it is assumed that the total energy of the system is zero. Having verified with other versions, it is concluded that the gravitational potential and kinetic energy are accurate. Knowing this, the strain energy can be derived from Equation 5.17.

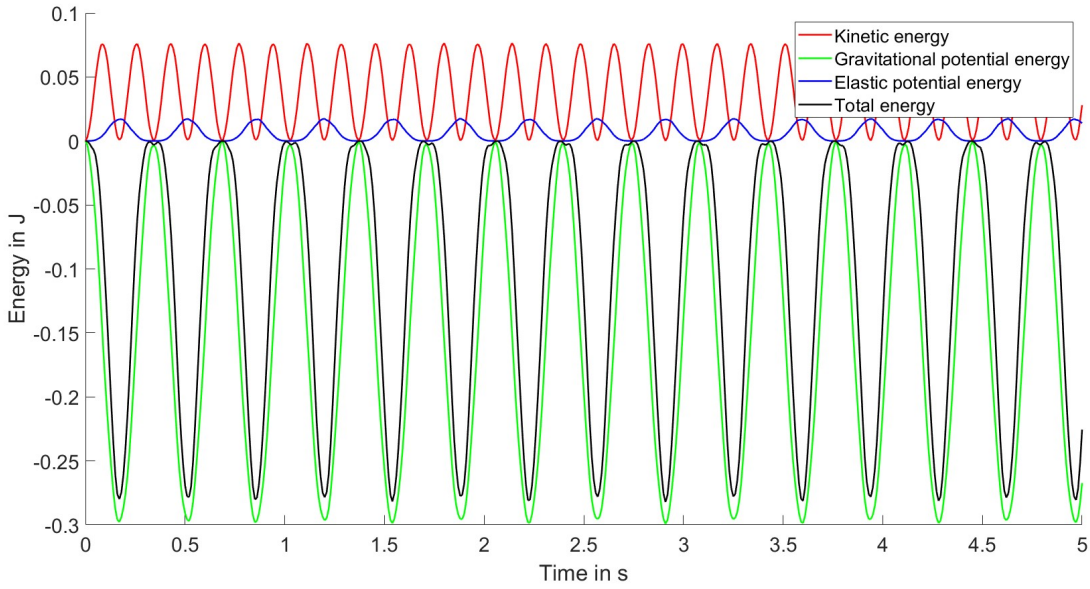

Figure 8: Example of the simulation results from a 12th order Chebyshev bases. The elastic energy is not computed correctly which results in the total energy not being zero.

8.1 Energy comparison of FEM vs Global base functions

We use the model with FEM cubic basis functions as a reference of the energy when compared to global base functions Figure 9. This is due to the high accuracy of FEM, whereas the use of global base functions should theoretically lead to less accuracy but less computational time. The amount of elements is 10 and it will be using 5 Gauss quadrature points to evaluate the integrals over each element.

As a global basis, it is chosen to use up to 12th order Chebyshev polynomials with 25 Gaussian quadrature points.

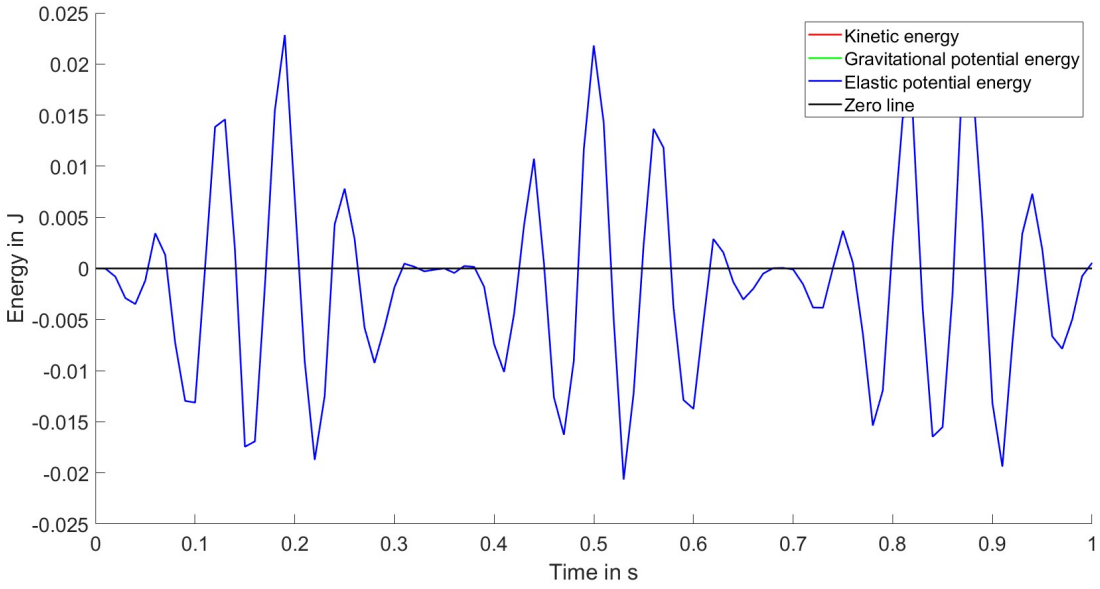

Figure 9: Plot of the energy difference between FEM cubic and 12th order Chebyshev basis functions over time

8.2 Bases order influences on the energy

For this case, it was looked at how the order of the bases have an impact on the energy. It was chosen to compare first, sixth and twelfth order Chebyshev polynomials bases with each other.

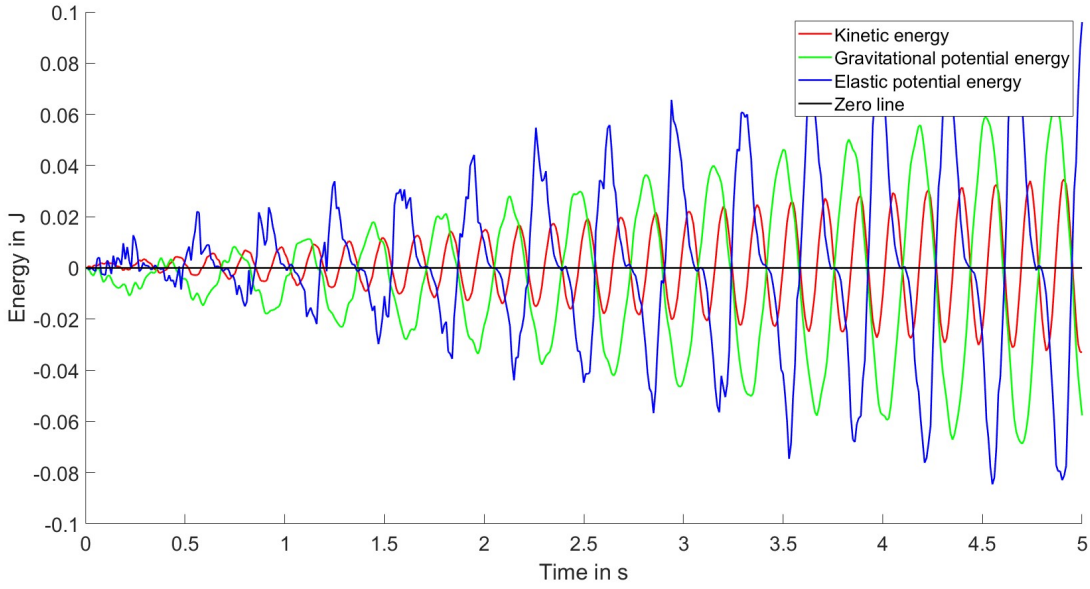

Figure 10: Plot of the energy difference between 1th and 6th order Chebyshev

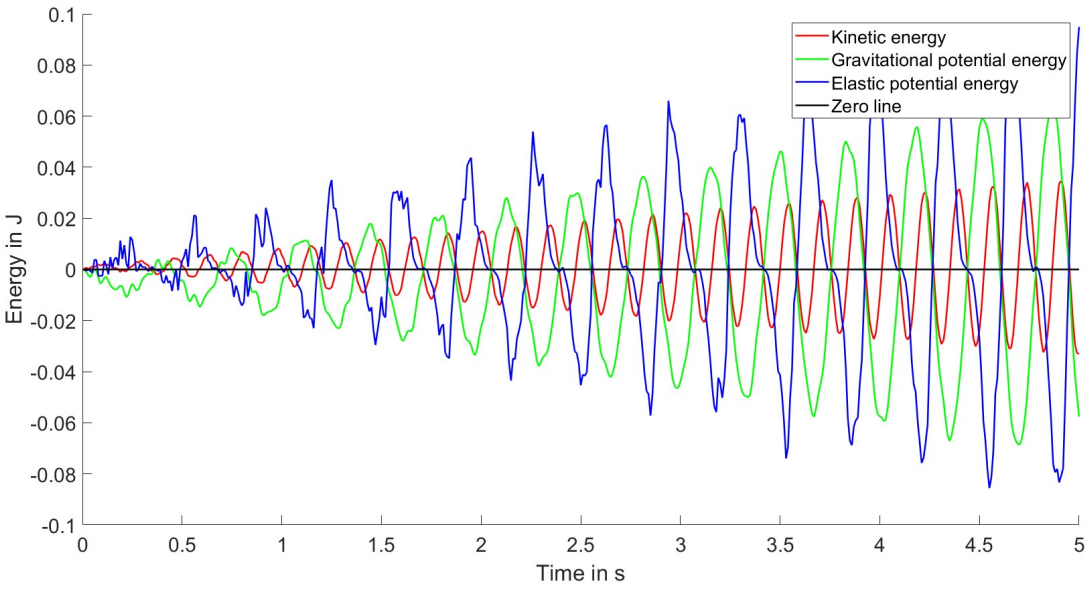

Figure 11: Plot of the energy difference between 1th and 12th order Chebyshev

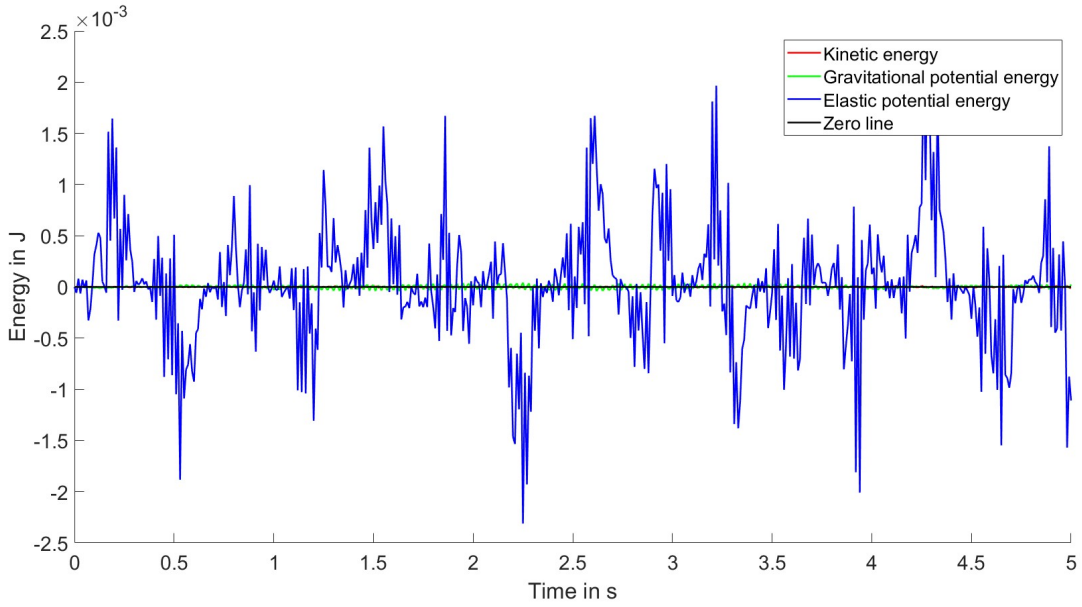

Figure 12: Plot of the energy difference between 6th and 12th order Chebyshev

8.3 Global bases influence on the energy

This section shows the results of the energy differences between bases from different polynomial families while maintaining the same order and amount of quadrature points.

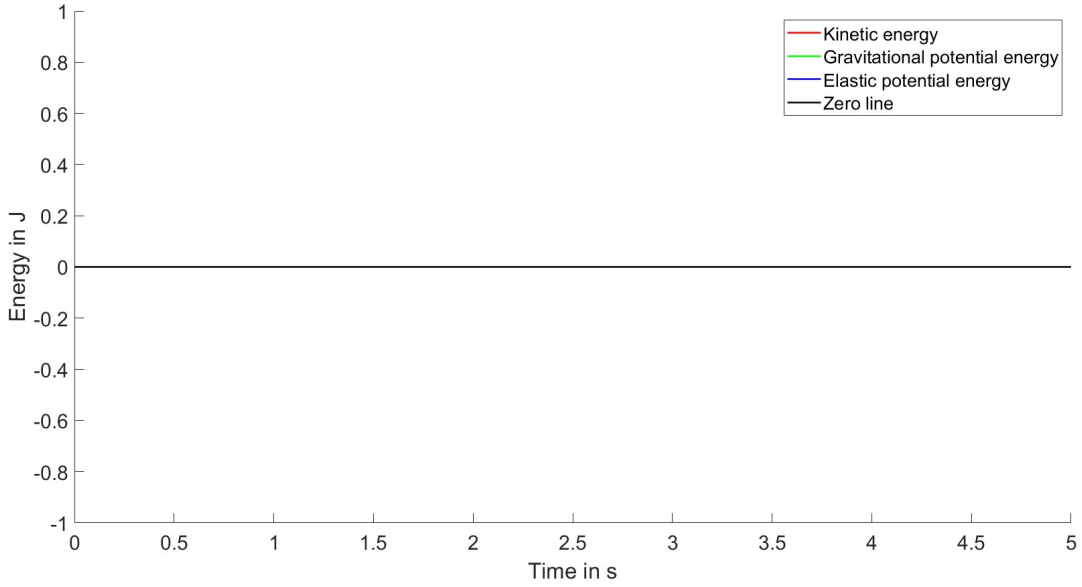

Figure 13: Plot of the energy difference between 6th order Chebyshev and 6th order Legendre

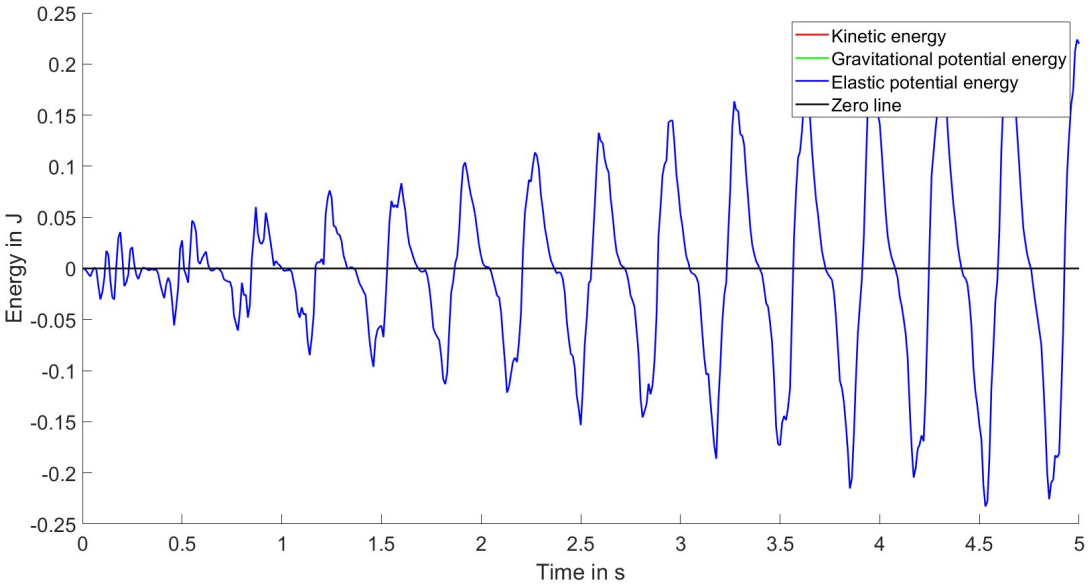

Figure 14: Plot of the energy difference between 6th order Chebyshev and 6th order Monomial

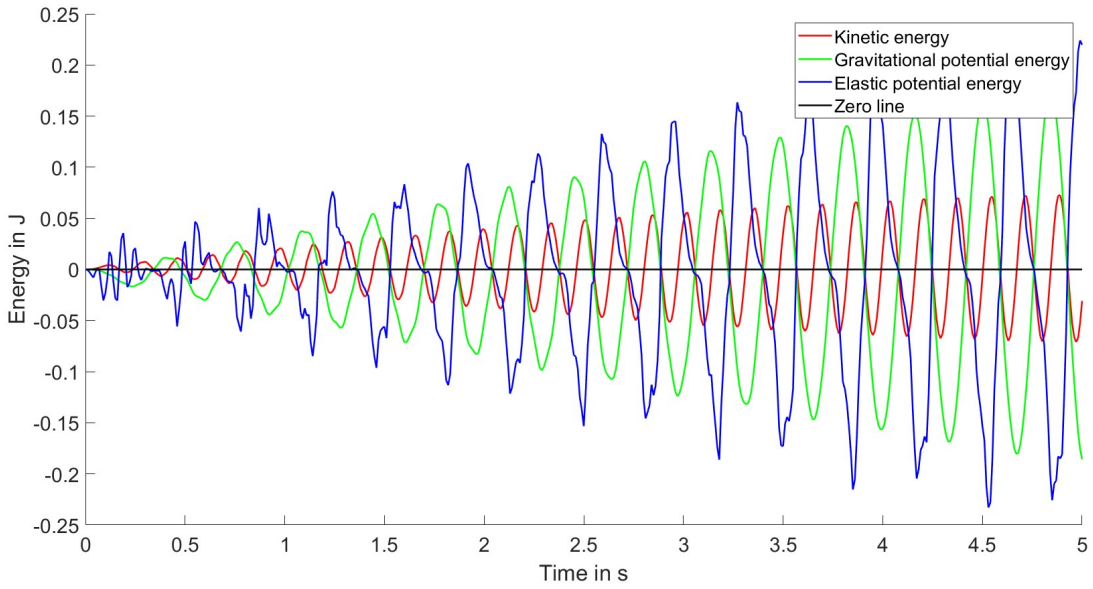

Figure 15: Plot of the energy difference between 6th order Chebyshev and 6th order Fourier

8.4 Influences of the Zanna order on the energy

In chapter 6 it was discussed how the Magnus expansion can be approximated through the Zanna collocation method. The expression of a fourth order Zanna approximation is stated in Equation 6.12). However, one can choose to also go for a second order approximation in which only one strain value is needed between two Gaussian points instead of two as shown in Figure 6. This reduces computation time at the cost of accuracy. A comparison between the two orders have been made and the resulting energy differences are shown in Figure 16.

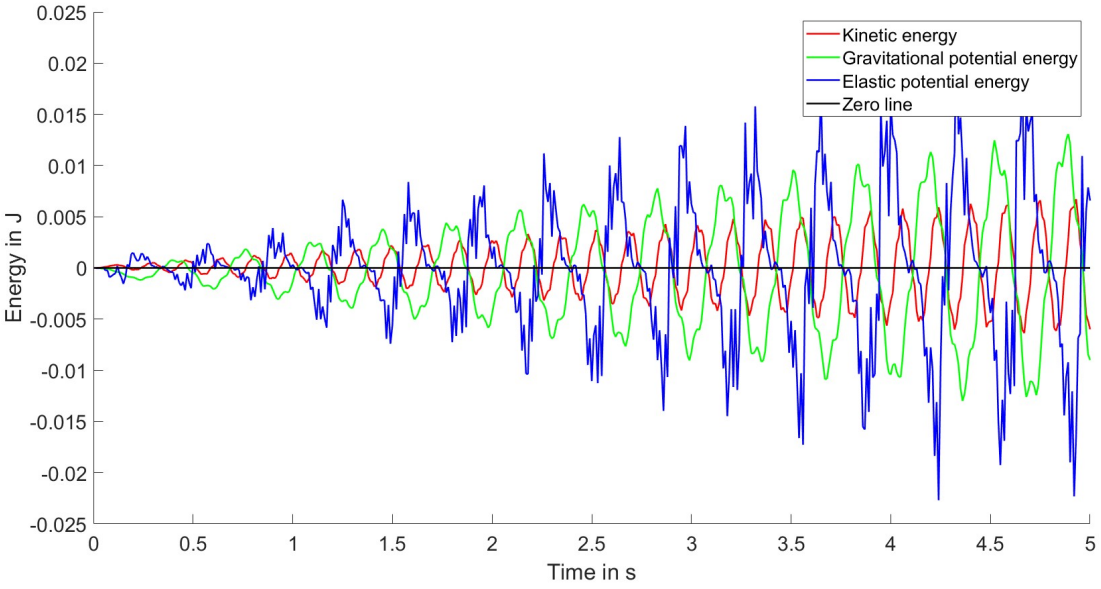

Figure 16: Plot of the energy difference between a simulation with a 4th order Zanna approximation and a 2nd order

9 Conclusion and future work

9.1 Conclusion

Throughout this thesis, we tried to find an answer to the following research question:

How is the energetic consistency of the Cosserat rod model affected by discretization?

In order to answer this question, the main question was split up into two sub-questions:

1. How can the continuous model be formulated?

2. How can the model be discretized?

It was chosen to go for a strain parameterized approach since it abides by a principle bundle structure which has the advantage to make a clear distinction between the external degrees of freedom and the internal degrees of freedom. Through this, the kinematics were formulated and the dynamics were obtained by Hamilton's least action principle. The recovery of the configuration through the strain is not a trivial matter; the Magnus expansion was needed.

The model can be discretized through first reducing the model by assuming that the strain field can be approximated by a finite set of basis functions and then be calculated through a Gauss quadrature rule. The Magnus expansion is approximated through the Zanna collocation method.

In chapter 8.1 we have seen that the local FEMlike and Chebyshev bases functions differ in elastic energy when compared to one another. The influence on the bases order for Chebyshev polynomials were shown in chapter 8.2, where a large energy differences are shown between 1st and 6th order Chebyshev polynomials and 1st and 12th order Chebyshev polynomials. It is interesting to note that the energy differences between 6th and 12th Chebyshev polynomials were relatively minimal. This means that a faster simulation can be obtained by choosing a 6th order bases without having a great loss of simulation accuracy. In chapter 8.3 the differences between global bases functions were shown. It is interesting to see that there is no difference in energy at all when comparing a Chebyshev bases to a Legendre one. This might be due to the fact that both the polynomial families look greatly alike. When checking a Chebyshev bases to a Monomial one, there is only a difference in elastic potential energy. This is not the case when comparing a Chebyshev to a Fourier basis. Lastly, we indeed see that the order of the Zanna approximation method matters as it is shown in chapter 8.4.

9.2 Future work

Based on this thesis, one could continue to work on the following:

• As stated in chapter 7, the current version of the SoRoSim toolbox (v6.3) does not show a correct energy balance due to the strain energy being calculated incorrectly. Although it has been verified with earlier versions of the toolbox that the system shows energy conservation, there is still need for a proper fix of this calculation in order for the toolbox to show results with machine precision.

• In this thesis, the Magnus expansion was used in order to calculate the configuration of the rod. Through the Zanna collocation method, one can then approximate these series up to a certain order. However, the Magnus expanions is not the only way to retrieve the configuration; an other possibility would be to use the Fer expansion instead. Since this expansion can also be approximated by the Zanna method, it might be interesting to see if one type of expansion is more accurate than the other.

10 Appendix

10.1 Proof of the Variational Material twist and velocity twist

We follow the proof from [27]. In this, we only look at the velocity twist vector $T \in \mathbb{R}^6$ since exact same derivation holds when the time derivative is replaced by a spatial derivative.

We use the fact that the δ operator is commutative:

$$\delta \frac{\partial H}{\partial t} = \frac{\partial}{\partial t} \delta H \tag{10.1}$$

Define the field material variation of H as:

$$\delta \tilde{\zeta} = H^{-1} \delta H \tag{10.2}$$

The velocity twist is defined as:

$$\tilde{T} = H^{-1} \frac{\partial H}{\partial t} \tag{10.3}$$

Then by substituting the field material variation and velocity twist and using the fact that the variation of the element of $SE(3)$ can be written in terms of ζ:

$$\delta(HT) = \frac{\partial H \delta \zeta}{\partial t} \tag{10.4}$$

Applying integration by parts:

$$\delta H T + H \delta T = \frac{\partial H \delta \zeta}{\partial t} + H \frac{\partial \delta \zeta}{\partial t} \tag{10.5}$$

Once again, use the fact that $\delta H = H \delta \zeta$ and $\frac{\partial H}{\partial t} = HT$:

$$H \left(\delta \zeta T + \delta T \right) = H \left(T \delta \zeta + \frac{\partial \delta \zeta}{\partial t} \right) \tag{10.6}$$

Since H is on both sides, we can get rid of this term and rewrite it which leads to:

$$\delta T = \frac{\delta \zeta}{\partial t} + T \delta \zeta - \delta \zeta T \tag{10.7}$$

In this, we can recognize the commutator (see preliminaries) and denote the expression as follows:

$$\delta T = \frac{\delta \zeta}{\partial t} + [T, \delta \zeta] \tag{10.8}$$

References

[1] cyberne1, "1957 – "artificial muscle" – joseph laws mckibben (american)." https://cyberneticzoo.com/bionics/1957-artificial-muscle-joseph-laws-mckibben-american/, April 2012.

[2] A. Faustinoni, "Soft robotics: Examples, research and applications." https://robotics24.net/blog/soft-robotics-examples-research-and-applications/.

[3] B. T. S. Kim, C. Laschi, "Soft robotics: A bioinspired evolution in robotics." https://www.researchgate.net/publication/236198827_Soft_robotics_A_bioinspired_evolution_in_robotics, April 2013.

[4] K. Pugh, "An introduction to outer banks jellyfish, sea nettles and other stingers." https://islandfreepress.org/hatteras-island-features/an-introduction-to-outer-banks-jellyfish-sea-nettles-and-other-stingers/, June 2021.

[5] L. Burrows, "Tentacle robot can gently grasp fragile objects." https://seas.harvard.edu/news/2022/10/tentacle-robot-can-gently-grasp-fragile-objects.

[6] E. C. . F. Cosserat., "Théorie des corps déformables." https://www.nature.com/articles/081067a0, July 1909.

[7] X. H. M. L. . W. H. Longhui Qin, Haijun Peng, "Modeling and simulation of dynamics in soft robotics: a review of numerical approaches." https://link.springer.com/article/10.1007/s43154-023-00105-z.

[8] R. C. Hossain Samei, "A fast geometric framework for dynamic cosserat rods with discrete actuated joints." https://ieeexplore.ieee.org/document/10160301.

[9] S. Grazioso, "Geometric soft robotics: A finite element approach." http://www.fedoa.unina.it/12234/1/grazioso_stanislao_30.pdf.

[10] B. Caasenbrood, "Design, modeling, and control strategies for soft robots." https://pure.tue.nl/ws/portalfiles/portal/314251017/20240110_Caasenbrood_hf.pdf, 2024.

[11] Stramigioli, "The principal bundle structure of continuum mechanics." https://arxiv.org/pdf/2210.11537.pdf.

[12] R. Rashad, A. Brugnoli, F. Califano, E. Luesink, and S. Stramigioli, "Intrinsic nonlinear elasticity: An exterior calculus formulation." https://arxiv.org/pdf/2303.06082.pdf.

[13] B. Németh and R. Adhikari, "A geometric formulation of schaefer's theory of cosserat solids." https://arxiv.org/pdf/2309.14268.pdf.

[14] F. C. F. R. F. Boyer, V. Lebastard, "Dynamics of continuum and soft robots: a strain parametrization based approach." https://hal.science/hal-02318617/document, 2020.

[15] M. P. F. Boyer, "Multibody system dynamics for bio-inspired locomotion: from geometric structures to computational aspects." https://iopscience.iop.org/article/10.1088/1748-3190/10/2/025007/pdf, March 2015.

[16] Boyer, "Poincare-chetayev equations and flexible multi-body systems." https://hal.science/hal-00672477.

[17] R. Hollander, "The magnus expansion." https://fse.studenttheses.ub.rug.nl/14905/1/BSc_Mathematics_2017_Hollander_RM.pdf.

[18] V. L. F. C. F. Renda, C. Armanini, "A geometric variable-strain approach for static modeling of soft manipulators with tendon and fluidic actuation." https://www.researchgate.net/publication/340466408_A_Geometric_Variable-Strain_Approach_for_Static_Modeling_of_Soft_Manipulators_With_Tendon_and_Fluidic_Actuation, April 2020.

[19] A. L. F. Boyer, M. Porez, "Poincaré–cosserat equations for the lighthill three-dimensional large amplitude elongated body theory: Application to robotics." https://hal.science/hal-00630754/document, 2010.

[20] A. P. Brandon Caasenbrood and H. Nijmeijer, "Energy-based control for soft manipulators using cosserat-beam models." https://www.scitepress.org/PublishedPapers/2021/105815/105815.pdf.

[21] A. Y. F. B. F. R. Anup Teejo Mathew, Daniel Feliu-Talegon, "Reduced order modeling of hybrid soft-rigid robots using global, local, and state-dependent strain parameterization." https://journals.sagepub.com/doi/10.1177/02783649241262333.

[22] L. W. Y. L. W. Q. K. Dow, S. Adeeb, "Numerical integration: Gauss quadrature." https://engcourses-uofa.ca/books/numericalanalysis/numerical-integration/gauss-quadrature/.

[23] C. A. F. B. A. T. Mathew, I. M. B. Hmida and F. Renda, "Sorosim: A matlab toolbox for hybrid rigid-soft robots based on the geometric variable-strain approach." IEEE Robotics Automation Magazine, doi: 10.1109/MRA.2022.3202488.

[24] N. S. A.L. Orekho, "Solving cosserat rod models via collocation and the magnus expansion." https://arxiv.org/abs/2008.01054, Augustus 2020.

[25] A. Zanna, "Collocation and relaxed collocation for the fer and the magnus expansions." https://www.researchgate.net/publication/243096220_Collocation_and_Relaxed_Collocation_for_the_Fer_and_the_Magnus_Expansions, June 1999.

[26] T. M. Inc., "ode45." https://nl.mathworks.com/help/matlab/ref/ode45.html, 2024.

[27] F. C. F. R. Frédéric Boyer, Vincent Lebastard, "Extended hamilton's principle applied to geometrically exact kirchhoff sliding rods." https://www.sciencedirect.com/science/article/pii/S0022460X21005411.